Synthesis and Antitumor Activity of Quinonoid Derivatives of Cannabinoids

Natalya M. Kogan,[#] Ruth Rabinowitz,[‡] Paloma Levi,[‡] Dan Gibson,[#] Peter Sandor,[†] Michael Schlesinger,[‡] and Raphael Mechoulam*[,#]

Department of Medicinal Chemistry and Natural Products, School of Pharmacy, The Hebrew University, Jerusalem 91120, Israel, Department of Experimental Medicine and Cancer Research, School of Medicine, The Hebrew University, Jerusalem 91120, Israel and NMR Applications Laboratory, Varian Deutschland GmbH, D-64289 Darmstadt, Germany

Received February 18, 2004

Three cannabis constituents, cannabidiol (**1**), Δ^8-tetrahydrocannabinol (**3**), and cannabinol (**5**), were oxidized to their respective para-quinones **2**, **4**, and **6**. In the 1960s, the oxidized product **4** had been assigned a para-quinone structure, which was later modified to an ortho-quinone. To distinguish between the two possible quinone structures, a detailed NMR investigation was undertaken. The original para-quinone structure was confirmed. X-ray crystallography elucidated the structures of the crystalline **2** and **6**. All three compounds displayed antiproliferative activity in several human cancer cell lines in vitro, and quinone **2** significantly reduced cancer growth of HT-29 cancer in nude mice.

Introduction

Quinones of various chemical families serve as biological modulators,[1−3] and both natural and synthetic quinones are widely used as drugs.[4,5] Anthracyclines, a large group of quinonoid compounds produced by different strains of streptomyces, exert antibiotic and antineoplasic effects and are used to treat some forms of cancer.[5] The best known members of this family are daunorubicin and doxorubicin, the first identified anthracyclins.[6] Other quinones are also used as anticancer drugs. Mitomycin C and streptonigrin produced by streptomyces, and the synthetic epirubicin and mitoxantron are well-known examples.[7] Although these and other quinonoid compounds are effective in the treatment of many different forms of cancer, their side effects (the most severe being cumulative heart toxicity) limit their use.[8,9] The development of quinonoid compounds that display antineoplastic activity, but are less toxic, is a major therapeutic goal.

A large number of cannabinoids have been synthesized and tested in various in vitro and in vivo assays, including models of several diseases.[10−13] However, although cannabinoid quinones were prepared by our group already back in 1968, in connection with an investigation on the chemical basis of the Beam test (a color test for cannabinoids),[14] they have not been evaluated as medicinal agents. We report now that such quinones exhibit potent antineoplastic activity in vitro and at least one of them is also active in vivo.

Chemistry

We have reported that oxidation of cannabidiol (CBD) (**1**) by air in an alcohol solution in the presence of 5% potassium hydroxide over 24 h led to the formation of the hydroxyquinone **2** in about 5−10% yield.[14] We have now found that a slight change in the reaction conditions (lowering the temperature to 0 °C) raised the yield to ∼20% and brought the reaction time down to 3 h (when no more starting material was detected) (Scheme 1). The hydroxyquinone crystallized from heptane. We have previously reported that the quinone **2** cyclized to the para-quinone **4** under acid conditions.[14] Hodjat-Kashani et al.[15] have suggested, however, that **4** is an ortho-quinone. Their structural assignment was based on nuclear Overhauser effect (NOE) NMR data (see below). If indeed **4** is an ortho-quinone, then **2** may also be an ortho-quinone. We have now confirmed by X-ray crystallography the structure of **2**, originally proposed by our group. The X-ray data are submitted as Supporting Information. Quinone **2** was code-named HU-331 (HU = Hebrew University).

Scheme 1. Synthesis of Compounds **2**, **4**, and **6**

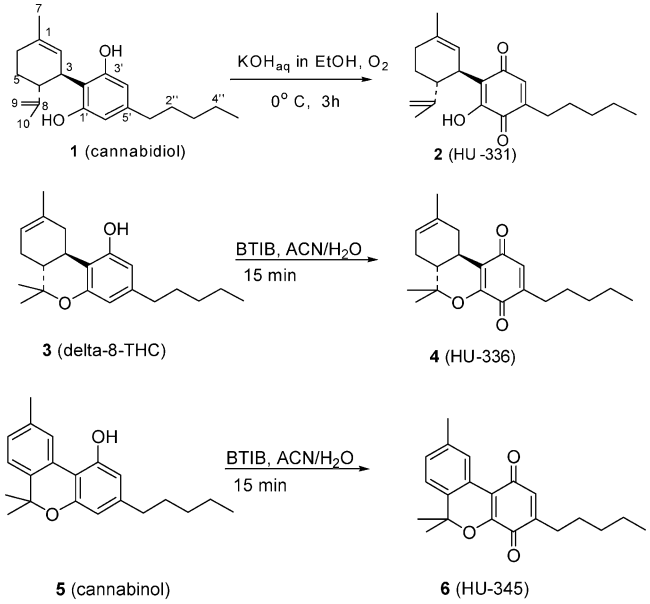

Oxidation of Δ^8-tetrahydrocannabinol (**3**) with *m*-chloroperbenzoic acid as originally reported[14] gave the

* To whom correspondence should be addressed. Phone: 972-2-6758634. Fax: 972-2-6757076. E-mail: mechou@cc.huji.ac.il.
[#] School of Pharmacy, The Hebrew University.
[‡] School of Medicine, The Hebrew University.
[†] NMR Applications Laboratory.

10.1021/jm040042o CCC: $27.50
Published on Web 06/10/2004

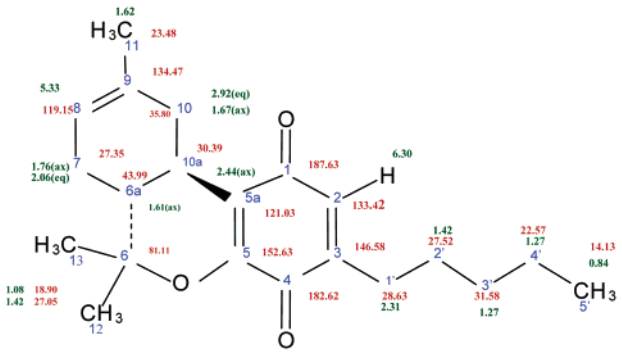

4

Figure 1. Structure of compound **4** with the atom labeling scheme and the proton and carbon chemical shifts.

desired quinone (**4**) in a low yield. To improve the yield, we now oxidized **3** with bis(trifluoroacetoxy)iodobenzene (BTIB), an oxidizing agent, which was not available when the original reaction was performed.

BTIB was first used for oxidation of phenols to quinones in 1989[16] and since then has become a widely used reagent for the oxidation of phenols to quinones.[17−20] BTIB oxidation of Δ^8-THC (**3**) led to the desired quinone **4** in 30−35% yield (Scheme 1). The compound was code-named HU-336.

An interesting feature of the oxidation of **3** is that by adding copper chloride in acetonitrile, which commonly leads to the formation of ortho-quinones,[21] the same para-quinone **4** is obtained as with BTIB and at approximately the same yield.

As mentioned above, we originally put forward a para-quinone structure for **4**,[14] while Hodjat-Kashani et al. proposed an ortho-quinone structure.[15] To establish the correct structure, a detailed NMR analysis was performed (see below). We have now established that compound **4** is indeed a para-quinone as originally suggested.

The quinone of cannabinol (CBN) (**6**), like the quinone of Δ^8-THC (**4**), was synthesized by oxidation with BTIB, with a yield of ~60%. The structure was determined by X-ray crystallography (data submitted as Supporting Information). The compound was code-named HU-345.

NMR Analysis of Δ^8-Tetrahydrocannabinolquinone (4)

Assignment of the Proton Spectrum. The structure of **4**, the atom labeling scheme, and the proton and carbon chemical shifts are depicted in Figure 1. The 5′-methyl group was assigned on the basis of its integration (3H), chemical shift (0.84 ppm), and multiplicity (triplet). Methylene groups 1′−4′ were assigned from analysis of the correlation spectroscopy (COSY) and gradient heteronuclear single quantum coherence total correlation spectroscopy (GHSQC-TOCSY) data. H2 was assigned on the basis of strong NOESY cross-peaks to 1′ and 2′, its chemical shift (6.30 ppm) and its multiplicity, and a triplet with a 1.36 Hz coupling constant indicating long-range coupling to 1′. The assignment of the H2 resonance does not, however, allow us to determine whether the two carbonyls are ortho or para to each other (vide infra). The broad peak at 5.33 ppm was assigned to H8 on the basis of its chemical shift. The remaining resonances of the spin system (H7, H6a, H10a, and H10) were assigned on the basis of standard analysis of COSY, NOESY, TOCSY, and GHSQC [for a review, see ref 22]. The methyl group 11 was assigned on the basis of a COSY cross-peak to H8 and of NOESY cross-peaks to H8 and H10. No attempt was made to distinguish between the methyl groups 12 and 13 (resonating at 1.08 and 1.42 ppm).

Assignment of the Carbon Spectrum. The protonated carbons were assigned by analysis of the HSQC spectrum in a straightforward manner. The assignments of the two nonequivalent protons of H10 (2.92 and 1.67 ppm) were confirmed by their cross-peaks to the same carbon resonance (35.80 ppm). Similarly, the two nonequivalent protons of H7 (2.06 and 1.76 ppm) were confirmed by cross-peaks to the same carbon resonance (27.35 ppm). C3 was assigned on the basis of cross-peaks to H2, H1′, and H2′ in the HMBC spectrum. C5 was assigned on the basis of its low-field chemical shift (152.63 ppm) and its HMBC cross-peaks to H10a (2.44 ppm) and to the methyl group at 1.42 ppm. C9, C6, and C5a were assigned on the basis of the analysis of the HMBC spectrum. The two carbonyls have resonances at 182.62 and 187.63 ppm.

Determining the Correct Constitution. We adopted a two-pronged approach: (a) to carry out a detailed high-field NMR study of **4** to sort out the correct positioning of two carbonyl groups and (b) to chemically reduce its two carbonyl groups and then form the corresponding acetates, which would provide us with two additional methyl groups to help determine the constitution by NOE studies.

We had hoped that the HMBC experiments that show long-range C−H correlations (two to four bonds) will be sufficient to sort out the question of the correct constitution. In practice, the proton at 6.30 ppm had strong correlations with C1′, C5a, and the carbonyl at 182.62 and weaker correlations with C3 and C5. Since the intensity, and even the observation of HMBC cross-peaks, is not merely a function of the number of bonds separating the two interacting nuclei but also depends on other structural factors (torsional angles and bond order), the data did not allow us to arrive at an unambiguous determination of the constitution. Thus, we decided to carry out a further experiment to determine carbon−carbon connectivity. We used the 1,1-adequate pulse sequence[23,24] detecting C13 single quantum coherences in the indirect domain. The resulting spectrum is similar to that of an HMBC except that only two-bond $^{13}C-^{1}H$ correlations are obtained. The cross-peaks of the resonance at 6.30 ppm are depicted (see Supporting Information), clearly demonstrating that the protonated carbon at 133.42 ppm is adjacent to C3 (146.58 ppm) and to a carbonyl at 187.63 ppm. This result is only consistent with the para structure where the protonated carbon C2 is between an sp^2 carbon and a carbonyl carbon. This experiment further confirms the assignment of the ^{13}C resonance at 187.63 ppm as C1. If the constitution were indeed ortho, the protonated carbon (C4) would have correlations to C3 (146.58 ppm) and to C5 (152.63 ppm) and there would be no correlation with a carbonyl carbon. The results of the adequate experiment prove beyond doubt that the positioning of the carbonyl groups is indeed para. The adequate

Scheme 2. Reductive Acetylation of **4**

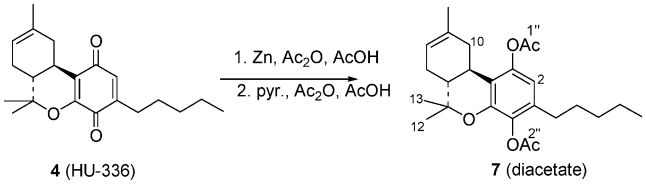

spectrum did confirm all of our previous ^{1}H and ^{13}C assignments.

To ensure finally that **4** is a para-quinone, reductive acetylation with zinc and acetic anhydride was performed (Scheme 2). The two acetyl methyl groups resonate at 2.27 and 2.29 ppm. The methyl group at 2.27 ppm has NOESY cross-peaks to C11 (1.67 ppm) and a strong cross-peak to H2 (6.30 ppm) and was therefore assigned as CH3(1). The methyl group at 2.29 ppm has a strong NOESY cross-peak to the methyl group at H12 (1.31 ppm), suggesting that it is the 2″-acetate group.

An energy minimization of the structure in the ortho geometry revealed that the shortest distance between the acetyl protons in positions 1 and 2 to the methyl protons in positions 12 and 13 is 4.08 Å, which would show weak cross-peaks in the NOESY spectrum, while in the para position the distance is 2.5−3.2 Å (expected to result in stronger NOE cross-peaks).

Our data, measured on a Varian Inova 600 MHz spectrometer, suggest that the proton resonances for the 12-methyl group and the 2′-methylene group overlap, and we assume that perhaps the proximity of the chemical shifts (1.420 and 1.438 ppm, respectively), which was not properly resolved on the 300 MHz spectrometer (a 5.4 Hz difference), may have been the reason for mistaking[15] the NOE between H2 and H2′ for the NOE between H4 and the methyl group 12.

Biological Section

The ability of the cannabinoid quinones to inhibit cancer growth in vitro was assayed on some human cancer cell lines: Raji (Burkitt's lymphoma), Jurkat (T-cell lymphoma), SNB-19 (glioblastoma), MCF-7 (breast cancer), DU-145 (prostate cancer), NCI-H-226 (lung cancer), and HT-29 (colon cancer) (see Supporting Information). Compound **2** exerted an inhibitory effect on the in vitro growth of all seven lines of human cancer cells tested (see Supporting Information). The most striking inhibition by **2** was found in tests with the Raji and Jurkat lymphoma cells. An inhibition of about 50% of the growth of both lymphomas was obtained at a concentration of **2** as low as 0.2 μg/mL. A concentration of 1.56 μg/mL inhibited the growth of the lymphomas by over 80%. The most sensitive epithelial cancer cells were HT-29 colon cancer cells and MCF-7 mammary cancer cells. A concentration of 3.125 μg/mL inhibited the growth of these cancer cell lines by about 50%. Compound **6** inhibited the growth of Raji cells more effectively than that of the other cell lines tested (see Supporting Information). For the inhibition of the growth of Jurkat cells and of all other cell lines, a concentration of 12.5−25.0 μg/mL of **6** was required. Compound **4** had the weakest capacity to inhibit the growth of human cancer cell lines in vitro. **4** exerted a similar inhibitory effect on all cell types at concentrations over 12.5 μg/mL.

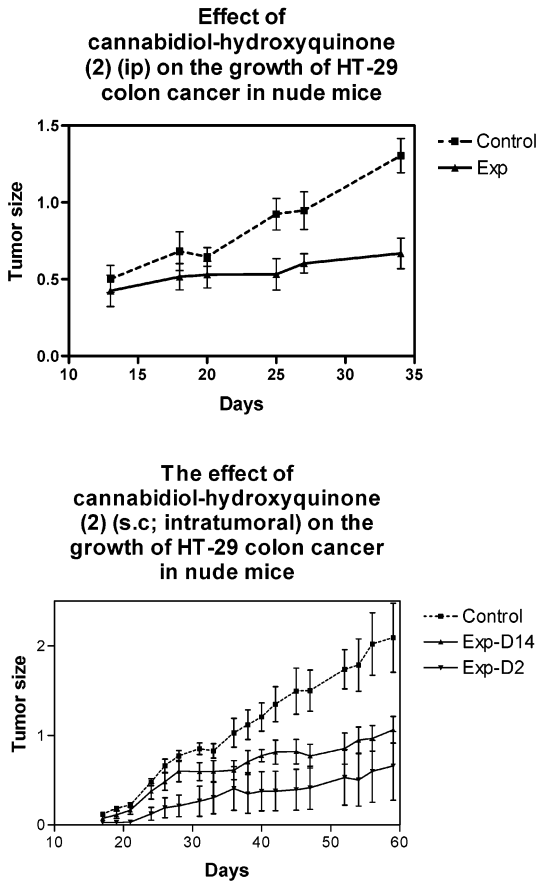

Figure 2. Results of in vivo action of **2** on HT-29 cancer growth: (Exp) injection of **2** from day 2 ip; (Exp-D2) injection of **2** from day 2 subcutaneously; (Exp-D14) injection of **2** intratumorally from day 14 after cancer cell injection.

It was of interest that the HT-29 and MCF-7 lines were most susceptible to inhibition by **2**, whereas the SNB-19 and DU-345 lines were more susceptible to inhibition by **4** and **6** than the other lines tested.

Experiments were carried out to determine the ability of **2** to inhibit the growth of human tumor cells in vivo. **2** was chosen for the in vivo assays because it was active at least against three cell lines (HT-29, Raji, and Jurkat) at doses considerably lower than those needed by **4** and **6**. Nude mice received a subcutaneous (sc) injection of HT-29 human colon cancer cells. At various time intervals after the administration of the tumor cells, the mice received three times per week intraperitoneal or subcutaneous injections of **2** at a dose of 5 mg/kg, which paralleled a concentration of 5 μg/mL in in vitro experiments, a concentration that killed about 50% of HT-29 cancer cells. Treatment of mice with **2** at a dose of 5 mg/kg did not cause either weight loss or any observable adverse effects in the treated mice. In one experiment (Figure 2) 10 nude mice, which received a sc injection of HT-29, were divided into two groups. Starting from day 2 after tumor injection, half of the mice received ip injections of **2**. The size of tumors was significantly smaller in mice injected with **2** than in vehicle-treated control mice, starting at 25 days after cancer cell injection ($p < 0.05$). At 35 days after cancer cell injection, the tumors in the treated group were half the size of the tumors in controls, a difference that was highly significant ($p < 0.0029$) (Figures 2 and 3).

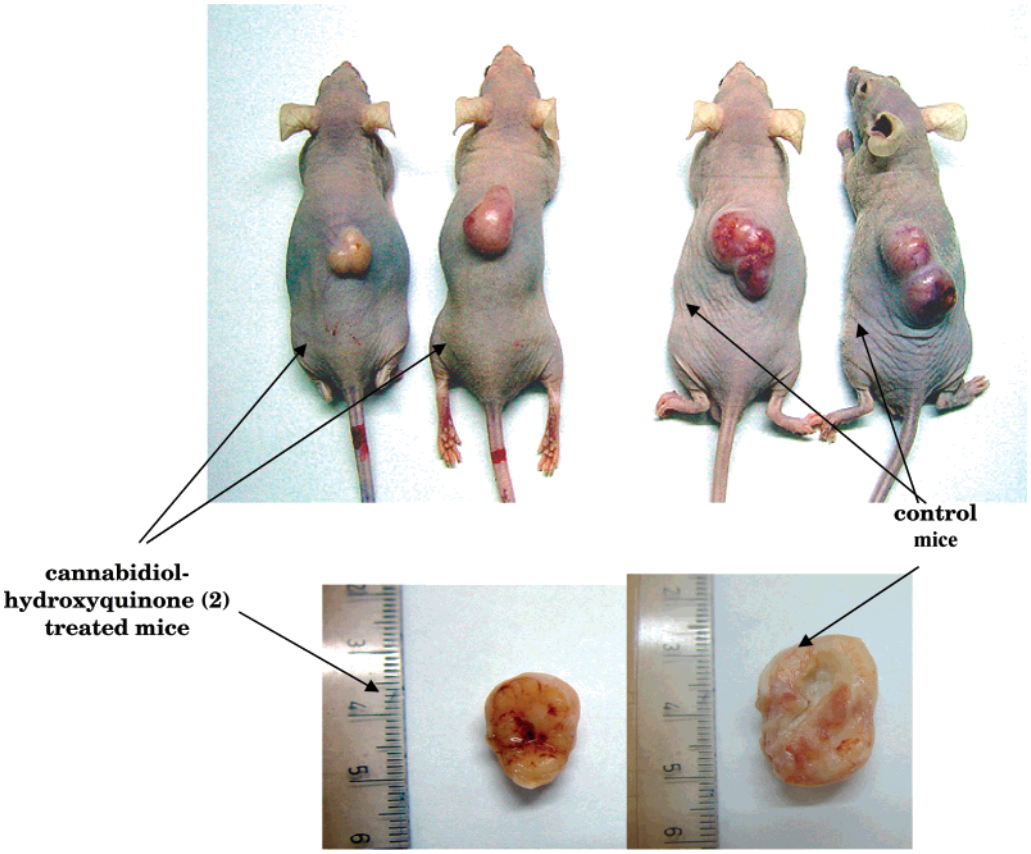

Figure 3. Effect of 5 mg/kg dose of **2** (ip) in vivo.

In another in vivo experiment, nude mice received an injection of HT-29 cancer cells subcutaneously in the back. **2** at a concentration of 5 mg/kg was likewise injected subcutaneously (Figure 2). In one group of nude mice, **2** was administrated intratumorally starting 14 days after the injection of tumor cells. In another group of nude mice, **2** was injected subcutaneously into the region where cancer cells were injected starting 2 days after the injection of tumor cells. In mice that received **2**, starting 2 days after tumor implantation, the tumor size was significantly smaller than in control mice at days 17−25 after tumor implantation and remained significantly smaller throughout the period of observation, till day 59 ($p < 0.05$). In mice that received **2** intratumorally starting 14 days after tumor implantation, the antitumor effect of **2** took a longer time to be manifested. The tumor size in treated mice was smaller than in controls from day 31 onward, but this difference was not significant until day 45 after cancer cell injection. Starting at day 45 after the cell injection and throughout the period of observation, the size of the tumors was significantly smaller than in control mice ($p < 0.05$).

In a further series of experiments, **2** was administered intraperitoneally at a dose of 2.5 mg/kg to nude mice that had received a subcutaneous implant of HT-29 cells 2 days earlier. The tumors developing in mice treated with **2** were smaller than in vehicle-treated control mice, but the difference was statistically significant only 39 days after tumor implantation (the area in cm^2 is 1.006 $\pm$ 0.1205 in the experimental group vs 1.893 $\pm$ 0.3154 in the control group; $p = 0.024$)

Conclusion

A large number of cannabinoids have been synthesized and tested in in vitro and in vivo models of diseases (for recent examples, see refs 13 and 25). Cannabinoids have been shown to inhibit the growth of tumor cells in culture and animal models.[26,27] They are usually well tolerated. However, cannabinoid-derived quinones have not been investigated in bioassays, although quinones of various chemical families are widely used as drugs. Cannabinoid-derived quinones were synthesized by our group in 1968, and they were assigned a para-quinone structure on the basis of UV spectroscopy.[14] In a later report, on the basis of an NMR study (NOE), it was concluded that the two carbonyls were in an ortho orientation.[15] We have now carried out a detailed NMR study in order to determine in an unequivocal way the correct positioning of the two carbonyl groups and confirmed the initially established structure of **4** as para-quinone. The structures of **2** and **6** quinones were established by X-ray crystallography.

The three cannabinoid quinones that were synthesized in our laboratory were tested for their antiproliferative activity on human cancer cell lines. All three compounds inhibited the in vitro growth of human cancer cell lines, albeit they differed in their potency. **4** exerted the weakest anticancer activity because concentrations of 12.5 μg/mL or higher were required to inhibit by 50% or more the growth of cells tested. The growth of SNB-19 cells was inhibited by **4** only at a concentration of 100 μg/mL. **6** was a more potent anticancer reagent than **4**. The growth of Raji lymphoma cells was inhibited by over 50% at a concentration of 6.25 μg/mL, while that of Jurkat lymphoma cells

and of DU-145 prostate cancer cells was inhibited by a concentration of 12.5 μg/mL. At concentrations of 25.0 μg/mL of **6**, all lines tested were inhibited. By far the most potent anticancer activity was displayed by **2**. An inhibition of 50% of the growth of the Raji and Jurkat lymphomas was obtained at a concentration of **2** as low as 0.2 μg/mL, while 50% inhibition of the growth of HT-29 colon cancer and of MCF-7 mammary cancer cells required a concentration of only 3.125 μg/mL. Further quinonoid derivatives of cannabinoids will have to be studied in order to determine the structure−activity relationships of these compounds.

Compound **2** displayed a marked anticancer activity not only in vitro but also in vivo in experiments with nude mice that received a subcutaneous inoculation of HT-29 colon carcinoma cells. The administration of **2** at a concentration that did not have observable adverse effects on the hosts (5 mg/kg) resulted in significant inhibition of the growth of the tumor cells when injected either intraperitoneally (ip) or subcutaneously (sc) into the region of the tumor graft. Often, compounds with anticancer activity are difficult to solubilize. The fact that **2** exerted a striking antitumor effect in vivo, following either sc or ip administration, indicates that the vehicle chosen for its solubilization (composed of 1:1:18 ethanol/emulphor/PBS (phosphate buffered saline)) enabled its bioavailability at the cancer site.

Many compounds containing quinone groups display potent anticancer activity (for a recent example, see ref 28 and references therein). A number of mechanisms have been suggested by which quinones may exert cell damage. These include redox cycling, DNA damage, and inhibition of topoisomerase, protein damage, and lipid peroxidation.[29] Similar mechanisms were shown to mediate the antitumor effects of adriamycin and daunorubicin, which have been in clinical use for the treatment of solid tumors for over 30 years.[30] The mechanism of the anticancer activity of cannabinoid quinones is still unclear. It may differ from the mechanisms proposed for other cannabinoids that bind to the CB1 receptor[26,27] because compounds **2**, **4**, and **6** do not bind to this receptor (unpublished results). The present study indicates that cannabinoid quinones possess a potential for development into anticancer drugs that may prove to be effective not only against lymphoma cells but also against solid tumors.

Experimental Section

NMR Spectrometry. NMR data were collected on Varian Unity Inova 500 and 600 MHz spectrometers using the standard pulse sequences and processed with the VNMR software.

Mass Spectrometry. The samples were analyzed by GC−MS in a Hewlett-Packard G1800 A GCD system with HP-5971 gas chromatograph with an electron ionization detector. Ultra-low-bleed 5% phenyl capillary column (28 m × 0.25 mm (i.d.) × 0.25 μm film thickness) based on diphenylmethylsiloxane chemistry (HP-5MS; Agilent Technologies) was used.

X-ray Crystallography. Data were measured on an ENRAF-NONIUS CAD4 computer-controlled diffractometer. Cu Kα (λ = 1.541 78 Å) radiation with a graphite crystal monochromator in the incident beam was used. The standard CAD4 centering, indexing, and data collection programs were used. The unit cell dimensions were obtained by a least-squares fit of 24 centered reflections in the range of 20° < θ < 28°. Intensity data were collected using the $\theta-2\theta$ technique to a maximum 2θ of 110°. The scan width, $\Delta\theta$, for each reflection was 0.80 + 0.15 tan θ. An aperture with a height of 4 mm and a variable width, calculated as 2.0 + 0.5 tan θ (in mm), was located 173 mm from the crystal. Reflections were first measured with a scan of 8.24 deg/min. The rate of the final scan was calculated from the preliminary scan results so that the ratio $I/\sigma(I)$ would be at least 20 but the maximum scan time would not exceed 60 s. If in the preliminary scan $I/\sigma(I) < 2$, this measurement was used as the datum. Scan rates varied from 1.27 to 8.24 deg/min. Of the 96 steps in the scan, the first and the last 16 steps were considered to be background. During data collection, the intensities of three standard reflections were monitored after every hour of X-ray exposure. No decay was observed. In addition, three orientation standards were checked after 100 reflections to check the effects of crystal movement. If the standard deviation of the *h*, *k*, and *l* values of any orientation reflection exceeded 0.10, a new orientation matrix was calculated on the basis of the recentering of the 24 reference reflections. Intensities were corrected for Lorentz and polarization effects. All non-hydrogen atoms were found by using the results of the SHELXS-86 direct method analysis.[36] After several cycles of refinements (all crystallographic computing was done on a VAX9000 computer at The Hebrew University of Jerusalem, using the TEXSAN structure analysis software), the positions of the hydrogen atoms were calculated and added to the refinement process.

Chemical Synthesis. All chemical reagents were purchased from Sigma-Aldrich. Organic solvents were purchased from Bio-Lab (Jerusalem). Cannabinol (**5**) and cannabidiol (**1**) were extracted from Lebanese-grown hashish.[31] Δ^8-THC (**3**) was prepared from cannabidiol by boiling with *p*-toluenesulfonic acid in toluene.[32] For column chromatography, we used ICN silica TSC, 60 Å.

Synthesis of 2 in the Presence of KOH. CBD (1.0 g, 3.18 mmol) was dissolved in 90 mL of petroleum ether (40−60 °C bp), and 5% KOH_{aq} in ethanol (10 mL, 8.77 mmol) was added. The reaction mixture was stirred at 0 °C in an open beaker for 3 h; after that 5% HCl (25 mL) was poured into it. The organic layer was washed with sodium bicarbonate and water and dried ($MgSO_4$). Removal of the solvent under reduced pressure yielded a glassy oil (1.1 g). The brownish oil obtained was purified by column chromatography using a petroleum ether−diethyl ether (95:5) solution. After crystallization from heptane, 211.0 mg (0.64 mmol, 20.2% yield) of large brown crystals were obtained. $[\alpha]_D$ in EtOH: −110° (in concentrated 0.1% w/v). Mp 50−51 °C. MS, *m*/*z*: 328, 313, 311, 237, 204. ^{1}H NMR (DMSO-d_6): δ 10.396 (s, 1H, O*H*), 6.415 (t, 1H, J = 1.43 Hz, H-4′), 5.080 (s, 1H, H-2), 4.501 (br s, 1H, H-9), 4.442 (br s, 1H, H-9), 3.60 (m, 1H, H-3), 2.750 (dt, 1H, J = 11.61, 2.85 Hz, H-4), 2.306 (dt, 2H, J = 7.50, 1.48 Hz, H-1″), 2.170 (m, 1H, H-5), 1.950 (m, 1H, H-5), 1.770 (m, 1H, H-6), 1.670 (m, 1H,H-6), 1.670 (s, 3H, H-7), 1.546 (s, 3H, H-10), 1.425 (q, 2H, J = 7.50 Hz, H-2″), 1.263 (m, 4H, H-3″, H-4″), 0.849 (t, 3H, J = 6.93 Hz, H-5″). Anal. ($C_{21}H_{28}O_3$) C. H: calcd, 8.59; found, 9.02.

Synthesis of 4 in the Presence of CuCl. To a solution of Δ^8-THC (104.0 mg, 0.33 mmol) in 0.9 mL of acetonitrile (ACN) CuCl (5.5 mg, 0.06 mmol) was added. A thin current of air was bubbled through the mixture for 1.5 h, after which 50 mL of ether was added. The reaction mixture was washed with H_2O, dried ($MgSO_4$), and concentrated. The yellowish oil obtained was purified by column chromatography using petroleum ether−diethyl ether (95:5) solution. After crystallization from heptane, 33.0 mg (0.10 mmol, 30.5% yield) of very thin yellow needles were obtained. $[\alpha]_D$ in EtOH: −110° (in concentrated 0.22% w/v). Mp- 53−54 °C. MS, *m*/*z*: 328, 313, 285, 272, 229, 204. ^{1}H NMR ($CDCl_3$): δ 6.300 (t, 1H, J = 1.51 Hz, H-2), 5.330 (s, 1H, H-8), 2.920 (dd, 1H, J = 17.04, 4.74 Hz, H-10), 2.440 (td, 1H, J = 11.32, 5.24 Hz, H-10a), 2.310 (td, 2H, J = 7.44, 1.51 Hz, H-1′), 2.060 (d, 1H, J = 17.21 Hz, H-7), 1.760 (d, 1H, J = 17.21 Hz, H-7), 1.670 (m, 1H, H-10), 1.620 (s, 3H, H-11), 1.610 (m, 1H, H-6a), 1.438 (m, 2H, H-2′), 1.420 (s, 3H, H-12), 1.270 (m, 4H, H-3′, H-4′), 1.080 (s, 3H, H-13), 0.840 (t, 3H, J = 6.99 Hz, H-5′). Anal. ($C_{21}H_{28}O_3$) C,H.

Synthesis of 4 with BTIB. To a solution of Δ^8-THC (50.1 mg, 0.16 mmol) in acetonitrile/H_2O (6:1, 0.7 mL) a solution of BTIB (215.0 mg, 0.50 mmol) in 0.7 mL of ACN/H_2O (6:1) was added dropwise. The reaction mixture was stirred at room temperature for 15 min, neutralized with aqueous $NaHCO_3$ saturated solution, and extracted with diethyl ether. The organic layer was washed with H_2O, dried ($MgSO_4$), and concentrated. The yellowish oil obtained was purified by column chromatography using a petroleum ether−diethyl ether (95:5) solution. After crystallization from heptane, 16.8 mg (0.05 mmol, 31.9% yield) of very thin yellow needles were obtained.

Synthesis of 6 in the Presence of CuCl. To a solution of CBN (95.0 mg, 0.31 mmol) in 0.9 mL of ACN CuCl (10.8 mg, 0.11 mmol) was added. A thin current of air was bubbled through the mixture for 6 h, after which 50 mL of ether was added. The reaction mixture was washed with H_2O, dried ($MgSO_4$), and concentrated. The red oil obtained was purified by column chromatography using a petroleum ether−diethyl ether (93:7) solution. After crystallization from heptane, 15.0 mg (0.05 mmol, 15.0% yield) of very large red crystals were obtained. Mp 81−82 °C. MS, *m/z*: 324, 309, 281, 225, 128. ^{1}H NMR ($CDCl_3$): δ 8.190 (s, 1H, H-1), 7.170 (d, 1H, J = 7.74 Hz, H-8), 7.080 (d, 1H, J = 7.74 Hz, H-7), 6.480 (t, 1H, J = 1.51 Hz, H-2), 2.440 (td, 2H, J = 7.46, 1.51 Hz, H-1′), 2.180 (s, 3H, H-11), 1.700 (s, 6H, H-12, H-13), 1.540 (q, 2H, J = 7.46 Hz, H-2′), 1.350 (m, 4H, H-3′, H-4′), 0.910 (t, 3H, J = 6.99 Hz, H-5′). Anal. ($C_{21}H_{24}O_3$) C,H.

Synthesis of 6 with BTIB. To a solution of CBN (50.0 mg, 0.16 mmol) in ACN/H_2O (6:1, 0.7 mL) a solution of BTIB (215.0 mg, 0.5 mmol) in 0.7 mL of ACN/H_2O (6:1) was added dropwise. The reaction mixture was stirred at room temperature for 15 min, neutralized with aqueous $NaHCO_3$ saturated solution, and extracted with diethyl ether. The organic layer was washed with H_2O, dried ($MgSO_4$), and concentrated. The red oil obtained was purified by column chromatography using petroleum ether−diethyl ether (93:7) solution. After crystallization from heptane, 29.1 mg (0.09 mmol, 56.1% yield) of very large red crystals were obtained.

Reductive Acetylation of 4 to 7. 4 (16.9 mg, 0.05 mmol) was dissolved in a solution of Ac_2O (acetic anhydride) (0.7 mL) and AcOH (acetic acid) (0.7 mL). Zn (5.4 mg, 0.83 mmol) was added, and the mixture was boiled under reflux for 30 min. The residue was filtered off, pyridine (2.2 mL) was added to the filtrate, and the solution was left at room temperature overnight under an N_2 atmosphere. After that, the solution was poured into ice-cold 5% HCl, the organic layer was washed with $NaHCO_3$ and water, dried ($MgSO_4$), and concentrated. The red oil obtained was purified by column chromatography using a petroleum ether−diethyl ether (90:10) solution. The diacetate (10.0 mg, 0.02 mmol, 46.5% yield) was obtained as a yellow oil. MS, *m/z*: 414, 372, 330, 287, 262, 247, 209. ^{1}H NMR ($CDCl_3$): δ 6.440 (br s, 1H, H-2), 5.330 (br s, 1H, H-8), 2.700 (m, 1H, H-10), 2.650 (m, 1H, H-10a), 2.440 (n, 2H, J = 7.75 Hz, H-1′), 2.290 (s,3H, H-2″), 2.270 (s,3H, H-1″), 2.100 (m, 1H, H-7), 1.960 (m, 1H, H-10), 1.770 (m, 1H, H-7), 1.750 (m, 1H, H-6a), 1.680 (s, 3H, H-11), 1.518 (q, 2H, J = 7.75 Hz, H-2′), 1.360 (s, 3H, H-12), 1.295 (m, 4H, H-3′, H-4′), 1.080 (s, 3H, H-13), 0.880 (t, 3H, J = 6.87 Hz, H-5′). Anal. ($C_{25}H_{34}O_5$) C. H: calcd, 8.27; found, 8.19.

Biological Evaluation. Raji and Jurkat cells were suspended in RPMI 1640 medium, supplemented with 20% heat-inactivated fetal calf serum, 2 mM L-glutamine, 100 U/mL penicillin, and 0.01 mg/mL streptomycin at 37 °C in a 5% CO_2 humidified atmosphere. Other cell lines were suspended in RPMI 1640 medium, supplemented with 10% heat-inactivated fetal calf serum, 2 mM L-glutamine, 100 U/mL penicillin, and 0.01 mg/mL streptomycin at 37 °C in a 5% CO_2 humidified atmosphere.

Cell Proliferation Test. Aliquots of suspensions of cancer cells were dispensed at 200 μL volumes into wells of 96-well tissue culture plates at densities of 0.02×10^6 cells/well. Various concentrations of cannabinoid quinones were introduced into the wells, and their efficacy was tested 3 days after initiation of the cultures, using the 3-(4,5-dimethylthiazol-2-yl)-2,5-diphenyltetrazolium bromide (MTT) assay. The principle of this assay is that cells that survived following exposure to various compounds can reduce MTT to a dark-colored formazan, while dead cells are incapable of doing so. The assay was performed as described previously.[33−35] In each MTT assay, every concentration of the cytotoxic substance was tested in five replicates in microplate wells. Assays with every cell line were carried out in two to three repeated experiments. The inhibitory effect of various compounds was calculated as a percentage inhibition in comparison with the values obtained in untreated wells to which vehicle (ethanol 0.5%) was added.

In Vivo Experiments. Tumors were grafted into nude mice by sc flank inoculation of 0.2×10^6 HT-29 cells in RPMI 1640 medium without fetal calf serum. The animals were assigned randomly to various groups and injected ip, intratumorally, or sc from day 2 or 14 after cell injection with vehicle (1:1:18 ethanol/emulphor/phosphate buffered saline), 5 or 2.5 mg/kg of **2**. Tumors were measured with an external caliper, and their areas were calculated by multiplying the length of the tumors by their width.

Acknowledgment. We thank Professor H. Ben-Bassat for providing us with human cancer cell lines. We are grateful to Dr. Shmuel Cohen (Department of Inorganic Chemistry, The Hebrew University) for performing X-ray analyses. This work was supported in part by grants from the Israel Science Foundation and the U.S. National Institute of Drug Abuse (Grant DA 9789) (to R.M) and by a contribution of the Goldhirsch Foundation (to M.S.). R.M. is affiliated with the David R. Blum Center for Pharmacy at the Hebrew University.

Supporting Information Available: ^{1}H, adequate, HSQC and COSY NMR spectra for **4**, NOESY and ^{1}H NMR spectra for **7**, X-ray crystallography data for **2** and **6**, elemental analyses for **2**, **4**, **6**, and **7**, and MTT test results for **2**, **4**, and **6**. This material is available free of charge via the Internet at http://pubs.acs.org.

References

(1) Thomson, R. H. *Naturally Occurring Quinones*; Routledge, Chapman & Hall: London, 1987.
(2) Meganathan, R. Biosynthesis of Menaquinone (Vitamin K2) and Ubiquinone (Coenzyme Q): A Perspective on Enzymatic Mechanisms. *Vitam. Horm.* **2001**, *61*, 173−218.
(3) McIntire, W. S. Newly Discovered Redox Cofactors: Possible Nutritional, Medical and Pharmacological Relevance to Higher Animals. *Annu. Rev. Nutr.* **1998**, *18*, 145−177.
(4) Lee, K. H. Novel Antitumor Agents from Higher Plants. *Med. Res. Rev.* **1999**, *19*, 569−596.
(5) Begleiter, A. Clinical Applications of Quinone-Containing Alkylating Agents. *Front. Biosci.* **2000**, *5*, E153−E171.
(6) Di Marco, A.; Cassinelli, G.; Arcamone, F. The Discovery of Daunorubicin. *Cancer Treat. Rep.* **1981**, *65* (Suppl. 4), 3−8.
(7) Arcamone, F.; Cassinelli, G. Biosynthetic Anthracyclines. *Curr. Med. Chem.* **1998**, *5*, 391−419
(8) Zucchi, R.; Danesi, R. Cardiac Toxicity of Antineoplastic Anthracyclines. *Curr. Med. Chem.: Anti-Cancer Agents* **2003**, *3*, 151−171.
(9) Thomas, X.; Le, Q. H.; Fiere, D. Anthracycline-Related Toxicity Requiring Cardiac Transplantation in Long-Term Disease-Free Survivors with Acute Promyelocytic Leukemia. *Ann. Hematol.* **2002**, *81*, 504−507.
(10) Razdan, R. K. Structure−Activity Relationships in Cannabinoids. *Pharmacol. Rev.* **1986**, *38*, 75−149.
(11) Mechoulam, R.; Hanus, L.; Fride, E. Towards Cannabinoid Drugs−Revisited. *Prog. Med. Chem.* **1998**, *35*, 199−243.
(12) Barth, F.; Rinaldi-Carmona, M. The Development of Cannabinoid Antagonists. *Curr. Med. Chem.* **1999**, *6*, 745−55.
(13) Bagshaw, S. M.; Hagen, N. A. Medical Efficacy of Cannabinoids and Marijuana: A Comprehensive Review of the Literature. *J. Palliat. Care* **2002**, *18*, 111−122.
(14) Mechoulam, R.; Ben-Zvi, Z.,; Gaoni, Y. Hashish-13. On the Nature of the Beam Test. *Tetrahedron* **1968**, *24*, 5615−5624.
(15) Hodjat-Kashani, H.; Lambert, G.; Duffley, R.; Razdan, R. Hashish: Oxidation of Δ^8-Tetrahydrocannabinol (THC); Synthesis of Δ^8-THC-1,2-dione and 2-Hydroxy-Δ^8-THC. *Heterocycles* **1986**, *24*, 1973−1976.

(16) Tamura, Y.; Yakura, T.; Tohma, H.; Kikuchi, K.; Kita, Y. Hypervalent Iodine Oxidation of *p*-Alcoxy- and Related Phenols: A Facile and Efficient Synthesis of *p*-Quinones. *Synthesis* **1989**, 126−127.
(17) Akai, S.; Kita, Y. Recent Progress in the Synthesis of *p*-Quinones and *p*-Dihydroquinones through Oxidation of Phenol Derivatives. A Review. *Org. Prep. Proced. Int.* **1998**, *30*, 603−629.
(18) Barret, R.; Daudon, M. Oxidation of Phenols to Quinones by Bis-(trifluoroacetoxy)iodobenzene. *Tetrahedron Lett.* **1990**, *31*, 4871−4872.
(19) Kato, N.; Sugaya, T.; Mimura, T.; Ikuta, M.; Kato, S.; Kuge, Y.; Tomioka, S.; Kasai, M. Facile and Efficient Synthesis of 7,10-Dihydroxy-6*H*-pyrazolo[4,5,1-*de*] Acridin-6-one via Hypervalent Iodine Oxidation. *Synthesis* **1997**, 625−627.
(20) Barret, R.; Daudon, M. An Efficient Synthesis of Juglone. *Synth. Commun.* **1990**, *20*, 2907−2912.
(21) Capdevielle, P.; Maumy, M. Ortho-Hydroxylation Selective des Phenols: 2. Un Noveau Systeme Catalytique a Charactere Preparative (Selective Ortho Hydroxylation of Phenols. 2. A New Catalytic System for Preparation). *Tetrahedron Lett* **1982**, *23*, 1577−1580.
(22) Reynolds, W. F.; Enriquez, R. G. Choosing the Best Pulse Sequences, Acquisition Parameters, Postacquisition Processing Strategies, and Probes for Natural Product Structure Elucidation by NMR Spectroscopy. *J. Nat. Prod.* **2002**, *65*, 221−244.
(23) Köck, M.; Reif, B.; Griesinger, C.; Fenical, W. Differentiation of HMBC Two- and Three-Bond Correlations: A Method To Simplify the Structure Determination of Natural Products. *Tetrahedron Lett.* **1996**, *37*, 363−366.
(24) Reif, B.; Köck, M.; Kerssebaum, R.; Kang, H.; Fenical, W.; Griesinger, C. ADEQUATE, a New Set of Experiments To Determine the Constitution of Small Molecules at Natural Abundance. *J. Magn. Reson., Ser. A* **1996**, *118*, 282−285.
(25) Croxford, J. L. Therapeutic Potential of Cannabinoids in CNS Disease. *CNS Drugs* **2003**, *17*, 179−202.
(26) Guzman, M. Cannabinoids: Potential Anticancer Agents. *Nat. Rev. Cancer* **2003**, *3*, 745−755.
(27) Portella, G.; Laezza, C.; Laccetti, P.; De Petrocellis, L.; Di Marzo, V.; Bifulco, M. Inhibitory Effects of Cannabinoid CB1 Receptor Stimulation on Tumor Growth and Metastatic Spreading: Actions on Signals Involved in Angiogenesis and Metastasis. *FASEB J.* **2003**, *17*, 1771−1773.
(28) Kissau, L.; Stahl, P.; Mazitschek, R.; Giannis, A.; Waldmann, H. Development of Natural Product-Derived Receptor Tyrosine Kinase Inhibitors Based on Conservation of Protein Domain Fold. *J. Med. Chem.* **2003**, *46* 2917−2931.
(29) Ollinger, K.; Kagedal, K. Induction of Apoptosis by Redox-Cycling Quinones. *Subcell. Biochem.* **2002**, *36*, 151−70.
(30) Gewirtz, D. A. A Critical Evaluation of the Mechanisms of Action Proposed for the Antitumor Effects of the Anthracycline Antibiotics Adriamycin and Daunorubicin. *Biochem. Pharmacol.* **1999**, *57*, 727−741.
(31) Gaoni, Y.; Mechoulam, R. The Isolation and Structure of Δ^1-THC and Other Neural Cannabinoids from Hashish. *J. Am. Chem. Soc.* **1971**, *93*, 217−224.
(32) Gaoni, Y.; Mechoulam, R. The Isomerisation of Cannabidiol to Tetrahydrocannabinoids. *Tetrahedron* **1966**, *22*, 1481−1488.
(33) Carmichael, J.; DeGraff, W. G.; Gazdar, A. F.; Minna, J. D.; Mitchell, J. B. Evaluation of a Tetrazolium-Based Semiautomated Colorimetric Assay: Assessment of Chemosensitivity Testing. *Cancer Res.* **1987**, *47*, 936−942.
(34) Rubinstein, L. V.; Shoemaker, R. H.; Paull, K. D.; Simon, R. M.; Tosini, S.; Skehan, P.; Scudiero, D. A.; Monks, A.; Boyd, M. R. Comparison of in Vitro Anticancer-Drug-Screening Data Generated with a Tetrazolium Assay versus a Protein Assay against a Diverse Panel of Human Tumor Cell Lines. *J. Natl. Cancer Inst.* **1990**, *82*, 1113−1118.
(35) Rubnov, S.; Kashman, Y.; Rabinowitz, R.; Schlesinger, M.; Mechoulam, R. Suppressors of Cancer Cell Proliferation from Fig (*Ficus carica*) Resin: Isolation and Structure Elucidation. *J. Nat. Prod.* **2001**, *64*, 993−996.
(36) Sheldrick, G. M. *Crystallographic Computing 3*; Oxford University Press: Oxford, U.K., 1985; pp 175−189.

JM040042O